# Multiple-Frequency and Variable-Temperature EPR Study of Gadolinium(III) Complexes with Polyaminocarboxylates: Analysis and Comparison of the Magnetically Dilute Powder and the Frozen-Solution Spectra

by **Meriem Benmelouka**[a]), **Johan Van Tol**[b]), **Alain Borel**[a]), **Saritha Nellutla**[b]), **Marc Port**[c]), **Lothar Helm***[a]), **Louis-Claude Brunel**[b])[d]), and **André E. Merbach**[a])

[a]) Institut des Sciences et Ingénierie Chimiques, Ecole Polytechnique Fédérale de Lausanne EPFL-BCH, CH-1015 Lausanne (fax: +41-21-6939895, email: lothar.helm@epfl.ch)

[b]) National High Magnetic Field Laboratory, Center for Interdisciplinary Magnetic Resonance, Florida State University, Tallahassee, Florida, USA

[c]) *Guerbet*, Research Department, 95943 Roissy Cdg Cedex, France

[d]) Present address: Center for Terahertz Science and Technology, Department of Physics, University of California, Santa Barbara, CA, USA

Dedicated to Prof. *Jean-Claude Bünzli* on the occasion of his 65th birthday in recognition of his prominent contribution to lanthanide chemistry

An electron paramagnetic resonance (EPR) study of glasses and magnetically dilute powders of $[Gd(DTPA)(H_2O)]^{2-}$, $[Gd(DOTA)(H_2O)]^{-}$, and macromolecular gadolinate(1−) complexes P792 was carried out at the X- and Q-bands and at 240 GHz (DTPA = diethylenetriaminepentaacetato; DOTA = 1,4,7,10-tetraazacyclododecane-1,4,7,10-tetraacetato). The results show that the zero-field splitting (ZFS) parameters for these complexes are quite different in a powder as compared to the frozen aqueous solution. In several complexes, an inversion of the sign of the axial component *D* of the zero field splitting is observed, indicating a significant structural change. In contrary to what was expected, powder samples obtained by lyophilization do not allow a more precise determination of the static ZFS parameters. The results obtained in glasses are more relevant to the problem of electron spin relaxation in aqueous solution than those obtained from powders.

**Introduction.** – In recent years, magnetic resonance imaging (MRI) has evolved into one of the most powerful diagnostic techniques in medicine, in part thanks to the application of suitable contrast agents. These paramagnetic pharmacological compounds function by increasing the relaxation rate of $H_2O$ protons in the surrounding tissue, due to the interaction of the proton spins with the electron spin of the complex. The majority of the currently used contrast agents are thermodynamically and kinetically stable gadolinium(III) chelates. This trivalent lanthanide ion has the highest possible number (seven) of unpaired electrons which makes it the most paramagnetic among the nonradioactive metal ions. The slow relaxation of the $Gd^{III}$ electron spin is an additional critical factor. The design of new, more efficient MRI contrast media requires a thorough understanding of all factors and mechanisms that influence relaxation enhancement of proton nuclear spins (relaxivity), and hence the efficiency of $Gd^{III}$ complexes [1].

Among other factors, the relaxivity is determined by *i*) the rotational diffusion of the complex, described by a correlation time $\tau_R$, *ii*) the chemical exchange of the $H_2O$ molecules directly bound to the metal with bulk $H_2O$ molecules (residence time $\tau_m$), and *iii*) the electronic spin relaxation times $T_{1e}$ and $T_{2e}$. While the molecular factors influencing *i* and *ii* are rather well understood [2–5], the electronic-spin relaxation of $Gd^{III}$ complexes relevant for MRI remains the subject of much discussion [6–15].

A general model for electronic relaxation of $Gd^{III}$ complexes in solution was presented by *Rast et al.* [8] where the electron-spin dynamics is determined by the rotation of a so-called static zero-field splitting (ZFS) and a modulation of a transient ZFS by random *Brownian* rotation of the complex and collisions with solvent molecules. Experimental EPR peak-to-peak line widths of several $Gd^{III}$ complexes were extracted from systematic measurements at variable temperature (0–100°), concentration, and frequency (9.44, 35, 75, 150, and 225 GHz) [9]. The data were interpreted by means of static ZFS parameters at second, fourth, and sixth order and a transient ZFS parameter at second order. While this improvement in theory is exciting, it contains a large number of parameters: four parameters for the amplitude of ZFS, two correlation times, and two activation energies describing their temperature dependence. An independent measurement of ZFS parameters will be useful. *Rast*'s model describes the transient ZFS modulation with an *Ornstein–Uhlenbeck* process [16], namely random jumps around an average value with a *Gaussian* probability distribution. This process is actually a dynamical equivalent to the *strain* encountered in the analysis of disordered solid-state EPR spectra [17][18]. *Gaussian* strain is a phenomenological description of a distribution of the spin-*Hamiltonian* parameters throughout the sample, for example due to differences in the H-bonding pattern around the spins. This model can be applied to the *g*-factor [19–21] (*g*-strain) and hyperfine coupling [22][23] (*A*-strain), as well as to the ZFS tensor [24–26] (*D*- and *E*-strain). Therefore, the determination of the ZFS parameters and their associated strains in the solid state provides us with an independent access to the key factors governing electron spin relaxation in $Gd^{III}$ complexes.

In addition to its importance in the context of multiple-frequency methods, high frequency EPR ($\nu > 90$ GHz) has a unique application as a single-frequency observation. In a previous study of frozen solutions of Gd-complexes, we have shown that measurements at very high frequency (240 GHz) and very low temperature ($T$ 4 K) allow to obtain values for the four parameters of the ZFS ($D$, $E$, $\sigma D$, and $\sigma E$). Furthermore, the technique allowed to determine directly from the EPR spectra the sign of the axial component $D$ for the chelating ligands studied: $D > 0$ for acyclic and $D < 0$ for cyclic ligands [27]. Experimental spectra of frozen solutions at higher temperatures could be simulated with the parameters determined at 4 K.

In this article, we first show that EPR spectra of frozen solutions at lower frequencies (X- and Q-band) can also be successfully simulated with the 4 K, 240 GHz-determined parameters. With the aim to determine more precisely the magnitude of the static ZFS by reducing as much as possible the transient component – which means strain –, we extend this EPR study to magnetically dilute powders of the DOTA and DTPA complexes (DOTA = 1,4,7,10-tetraazacyclododecane-1,4,7,10-tetraacetato(4–), DTPA = diethylenetriaminepentaacetato = *N*,*N*-bis{2-[bis(carboxymethyl)amino]ethyl}glycinato(5–)) and two mixtures of isomers of the macromolecular gadolinate(1–)

complex P792. The first, P792(R), is a mixture of six different stereoisomers arising from the configuration at each of the stereogenic C-atoms in the side chains (*i.e.*, the chiral (*R*,*R*,*R*,*R*), (*S*,*S*,*S*,*S*), (*R*,*S*,*S*,*S*), and (*S*,*R*,*R*,*R*) isomers and the achiral (*R*,*S*,*R*,*S*) and (*R*,*R*,*S*,*S*) diastereoisomers). The second mixture, P792(B), consists of the (*R*,*R*,*R*,*R*) and (*S*,*S*,*S*,*S*) isomers (*Fig. 1*).

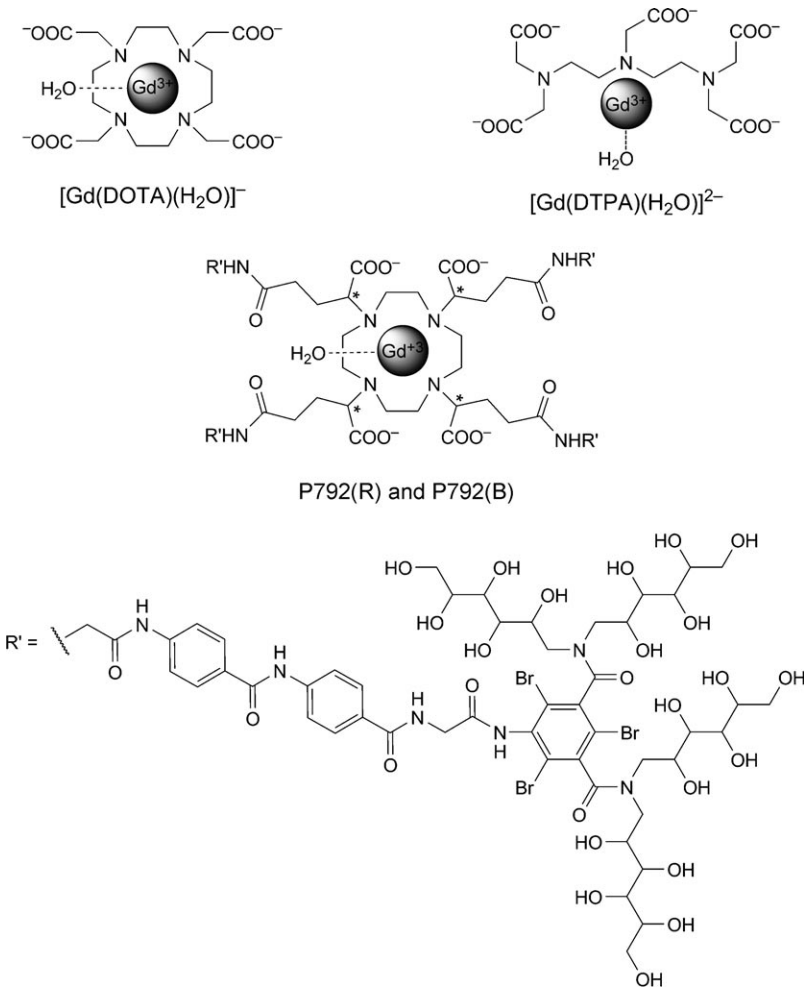


Fig. 1. *Molecular structures of [Gd(DOTA)(H$_2$O)]$^-$, [Gd(DTPA)(H$_2$O)]$^{2-}$, and Gadolinates(1 –) P792(R) and P792(B)*

**Experimental.** – 1. *Materials.* The DTPA and the DOTA ligands were purchased from *Sigma – Aldrich* and used without further purification. The gadolinate(1 –) powders P792(R) and P792(B) were supplied from *Guerbet Pharmaceuticals.*

2. *Samples Preparation.* The [Gd(DTPA)(H$_2$O)]$^{2-}$ and [Gd(DOTA)(H$_2$O)]$^-$ solns. were prepared *in situ* by dissolving the ligand (10% excess) in a aq. Gd(ClO$_4$)$_3$ soln. The pH was adjusted to 6.5 by

adding NaOH soln. All solns. were checked for the absence of free $Gd^{III}$ ion with the xylenol-orange test [28]. Final concentrations of 0.5 mM were prepared in glycerol/$H_2O$ 1:1. The glasses were formed by flash freezing the sample in liquid $N_2$ before loading into the precooled continuous-flow cryostat.

The magnetically dilute powders were prepared from an aq. soln. of $Y(ClO_4)_3/Gd(ClO_4)_3$ 99:1 (*w*/*w*) and DTPA or DOTA ligand. The samples were lyophilized with a *SpeedVac* concentrator. The solids obtained were finely ground to obtain a homogeneous powder. The gadolinate(1−) powders P792(B) and P792(R) [29] were used without any spin dilution because the dipolar interactions between the gadolinium ions are small in this case, due to the important molecular size of both P792 compounds.

3. *EPR Measurements.* The EPR spectra at 240 GHz were measured at the EPR facility of the National High Magnetic Field Laboratory with a home-built quasi-optical superheterodyne spectrometer [30]. A configuration without cavity was used, with a *Teflon* sample cup containing the powders. The photon energy of 240 GHz electromagnetic radiation corresponds to a temperature of 11.5 K. Therefore, at 4 K, almost only the transitions between the lowest-energy levels are observed. However, even at a very low irradiation power with a $B_1$ field smaller than 1 μT, the spectrum was distorted due to saturation. For that reason, at the lowest temperatures, rapid-passage EPR [31] was employed to record the spectra, by using relatively high power (*ca.* 1 mW at the sample, $B_1$ *ca.* 10 μT) and small modulation amplitudes. Instead of a derivative lineshape, the absorption lineshape was directly obtained. At temperatures above 30 K, standard CW-EPR was used. Lower-frequency EPR spectra were recorded at the X-band (9.44 GHz) and Q-band (*ca.* 34 GHz) with a *Bruker-ELEXSYS-E-500* spectrometer. CW-EPR was used at all frequencies.

4. *Data Analysis.* The EPR spectra were simulated and fitted with a home-written program EPRcalc [29][32], which utilizes complete diagonalization of the effective spin *Hamiltonian*, which can be expressed by *Eqn. 1*, with $S = 7/2$. The first term represents the field-dependent electron *Zeeman* contribution and the second and third terms, without any explicit $B_0$ dependence, represent the zero-field splitting. The parameter $\vec{\tilde{g}}$ is the *Zeeman*-splitting tensor, $\mu_B$ the *Bohr* magneton, and $B_0$ the external magnetic field. *D* and *E* are the axial and rhombic ZFS coefficients, which describe the deviation from the octahedral and the axial symmetry, resp.

$$\hat{H} = \mu_B \hat{S} \cdot \vec{\tilde{g}} \cdot \vec{B} + D(\hat{S}_z^2 - \hat{S}^2/3) + E(\hat{S}_x^2 - \hat{S}_y^2) \tag{1}$$

The distributions of *D* and *E*, in the frozen solutions and the powders, are noted *D*-strain ($\sigma D$) and *E*-strain ($\sigma E$) and are assumed to be *Gaussian* and given by *Eqn. 2*. They are accounted for by including a *Gaussian* line-broadening that is proportional to the shift of the transitions due to a change in *D* and *E*. No correlation between $\sigma D$ and $\sigma E$ is assumed.

$$P(D_i) \sim e^{-\left[\frac{2(D_i - D)}{\sigma D}\right]^2}; \quad P(E_i) \sim e^{-\left[\frac{2(E_i - E)}{\sigma E}\right]^2} \tag{2}$$

Higher-order terms in the ZFS and the terms arising from the nuclear interactions – nuclear hyperfine, nuclear *Zeeman*, superhyperfine, and quadrupole interactions – are neglected.

**Results and Discussion.** – As it was underlined in the previous EPR study of $Gd^{III}$ complexes in frozen solutions (glasses) [27], recording EPR spectra at 240 GHz and very low temperatures (below 150 K) allows a direct and straightforward determination of the parameters governing the strength of ZFS. Furthermore, it provided us with an elegant way to determine the sign of the axial ZFS parameter *D*. A correlation was established between the sign of *D* and the nature of the chelating ligand in the studied $Gd^{III}$ complexes: positive and negative signs were observed for acyclic (*e.g.*, DTPA) and marcocyclic (*e.g.*, DOTA) complexes, respectively. *Fig. 2* [27] shows experimental and calculated EPR spectra of $[Gd(DTPA)(H_2O)]^{2-}$ and $[Gd(DOTA)(H_2O)]^{-}$ glasses at 240 GHz and 4 K. The sign of *D* is unequivocally

defined by the small, narrow peak due to the $-1/2 \rightarrow +1/2$ transition being at lower or higher field with respect to the maximum of the broad peak which at 4 K is mainly due to the $-7/2 \rightarrow -5/2$ transition. The four ZFS parameters $D$, $E$, $\sigma D$, and $\sigma E$ were determined from least-square fitting of the 4 K spectra. The validity of the fitted ZFS parameters was then confirmed by their ability to simulate the higher-temperature spectra at 240 GHz [27].

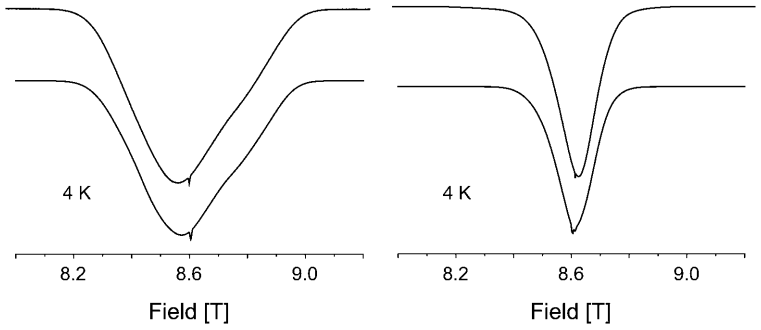


Fig. 2. *Experimental* (upper) *and fitted* (lower) *EPR spectra of* $[Gd(DTPA)(H_2O)]^{2-}$ (left) *and* $[Gd(DOTA)(H_2O)]^{-}$ (right) *in* $H_2O$*/glycerol glasses at 240 GHz* (taken from [27])

*Frozen Solutions*. With the aim to assess the soundness of the high-frequency results, further measurements and simulations for $[Gd(DTPA)(H_2O)]^{2-}$ and $[Gd(DOTA)(H_2O)]^{-}$ glasses were carried out at the Q- and X-bands. *Fig. 3* illustrates experimental and simulated spectra obtained with the high-field parameters of both complexes at these two bands at 160 K. Fitting the Q-band spectra by adjusting $D$, $E$, $\sigma D$, and $\sigma E$ leads only to a slight improvement of the agreement between the calculated and the experimental spectra, and the parameters obtained change less than 10%. However, using these fitted parameters to simulate the 240 GHz and 4 K data led to noticeable disagreement between the calculated and the experimental spectra. Therefore, we report only the spectra simulated at the Q- and X-bands with the 240 GHz and 4 K parameters defined previously [27] (*Table 1*). A fit of the X-band spectra was not possible because the approximation used to calculate the strain break down if the ZFS parameters are of the same order of magnitude as the observation frequency.

The comparison among spectra at different frequencies reveals certain important trends. At 240 GHz (*Fig. 2*), the $[Gd(DTPA)(H_2O)]^{2-}$ spectrum is about two times broader than that of $[Gd(DOTA)(H_2O)]^{-}$, a tendency which is retained at lower frequencies. Complex spectral features are observed at the X-band and to a minor extent at the Q-band for $[Gd(DTPA)(H_2O)]^{2-}$. In the simulations, these features are highly sensitive to changes in the ZFS parameters, especially $D$. For $[Gd(DOTA)(H_2O)]^{-}$, the spectra at the Q- and X-bands exhibit only small satellite peaks around one main sharp peak (*Fig. 3*). These spectra are less informative than the one obtained at 240 GHz. The difference in the apparent spectral width and the spectral complexity can be essentially explained by the larger magnitude of the ZFS

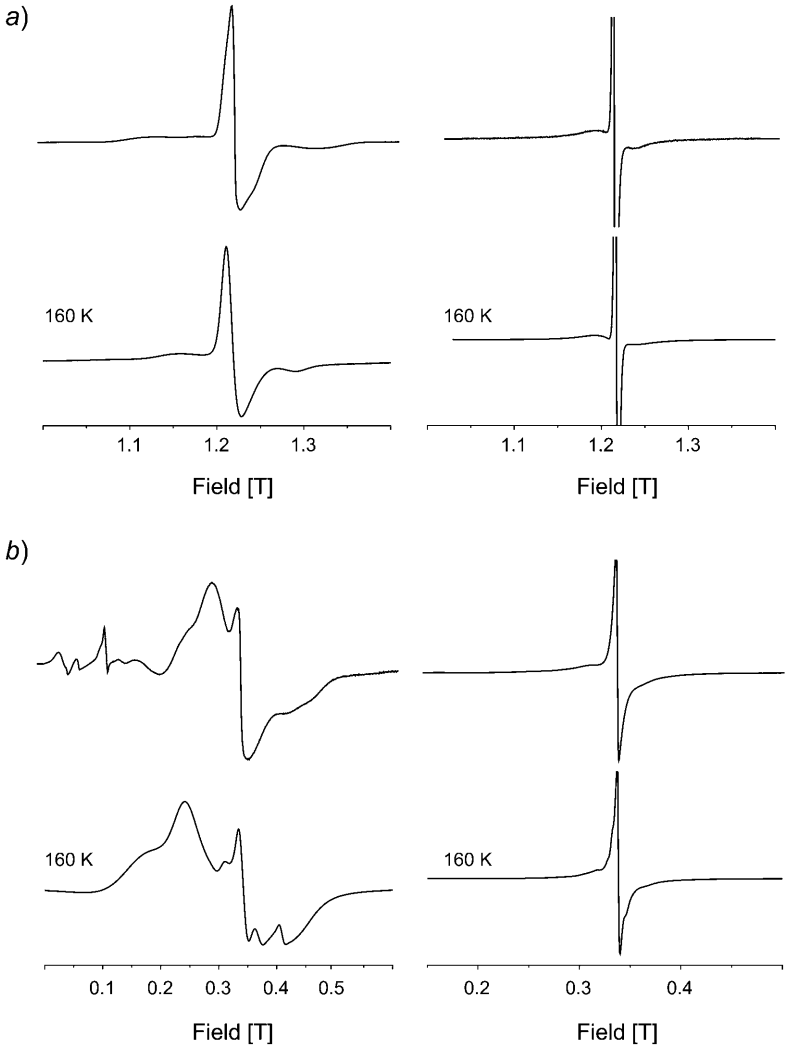


Fig. 3. *Experimental* (upper) *and simulated* (lower) *EPR spectra of [Gd(DTPA)(H$_2$O)]$^{2-}$* (left) *and [Gd(DOTA)(H$_2$O)]$^-$* (right) *in H$_2$O/glycerol glasses* a) *at the Q-band and* b) *at the X-band*

parameter $D$ for the acyclic $[Gd(DTPA)(H_2O)]^{2-}$ compared to the cyclic $[Gd(DOTA)(H_2O)]^-$.

*Powders.* EPR Spectra of magnetically dilute powders of $[Y(DTPA)(H_2O)]^{2-}$ and $[Y(DOTA)(H_2O)]^-$ with *ca.* 1% (*w*/*w*) of $Gd^{III}$ ion were measured at 240 GHz and at the Q- and X-bands from 5 K to 298 K (*Figs. 4* and *5*). The high-frequency and low-temperature powder spectra were fitted by the same procedure as for the frozen solutions by adjusting the four ZFS parameters $D$, $E$, $\sigma D$, and $\sigma E$. Spectra measured at the Q- and X-bands and at 298 K were only simulated and are represented in *Fig. 5*. The fitted parameters are reported in *Table 1*. The agreement of the fit to the experimental

Table 1. *The ZFS Parameters Obtained by Fitting the Experimental EPR Spectra of [Gd(DTPA)$H_2O$]$^{2-}$ and [Gd(DOTA)$H_2O$]$^-$ at 240 GHz of Glasses* (4 K) *and Powders* (5 K). Estimated error is equal to 0.002 $cm^{-1}$.

| | [Gd(DTPA)($H_2O$)]$^{2-}$ | | [Gd(DOTA)($H_2O$)]$^-$ | |
|---|---|---|---|---|
| | powder | glass[a]) | powder | glass[a]) |
| $D$ [$cm^{-1}$] | – 0.029 | 0.048 | 0.030 | – 0.019 |
| $E$ [$cm^{-1}$] | 0.004 | 0.013 | 0.006 | 0.000 |
| $E/D$ | – 0.14 | 0.27 | 0.20 | 0.00 |
| $\sigma D$ [$cm^{-1}$] | 0.005 | 0.022 | 0.026 | 0.019 |
| $\sigma E$ [$cm^{-1}$] | 0.001 | 0.007 | 0.004 | 0.013 |

[a]) [27].

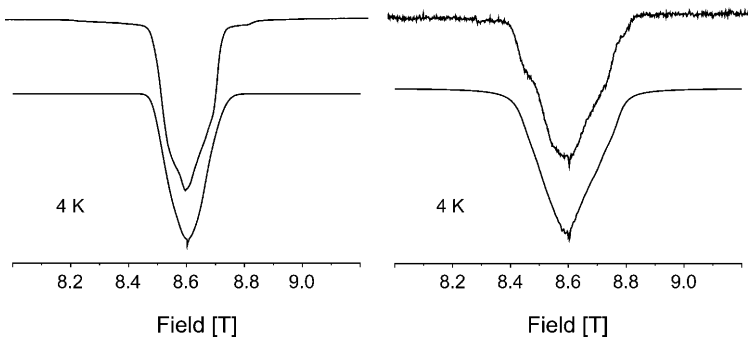


Fig. 4. *Experimental* (upper) *and fitted* (lower) *EPR spectra of magnetically dilute powders of [Y(DTPA)($H_2O$)]$^{2-}$* (left) *and [Y(DOTA)($H_2O$)]$^-$* (right) *with* ca. *1%* (w/w) *$Gd^{III}$ at 240 GHz*

data for the powders is not as good as for the frozen solutions. This is likely due to a non-*Gaussian* distribution of $D$ and $E$ values in the powder.

The results show that the sign of $D$ calculated from 4 – 5 K and 240 GHz spectra for both complexes is the opposite of the one obtained from glasses, a fact that can already be observed by comparing the spectra of glasses and powders (*Figs. 2 – 4*). The magnitudes of the ZFS parameters for the powders are also different from those obtained in frozen solutions [27]. A change in value of $D$ and $E$ is indicative of differences in the structure around the paramagnetic center. In the case of our powders, we observe a ZFS strain which is of the same magnitude as the average ZFS itself. The strain is often interpreted in terms of distribution of H-bonding throughout a disordered sample, yielding slightly different charge densities around each paramagnetic center [26]. Therefore, even small changes in the vicinity of the chelate molecules could lead to significant changes in $D$ and $E$, including a shift of its average values. In particular, when studying powders instead of liquid or frozen solutions, the replacement of well-organized second-shell $H_2O$ molecules by counter ions and/or the small excess of free ligand molecules could explain the observed changes between the measured powder and frozen-solution spectra and thus the calculated parameters.

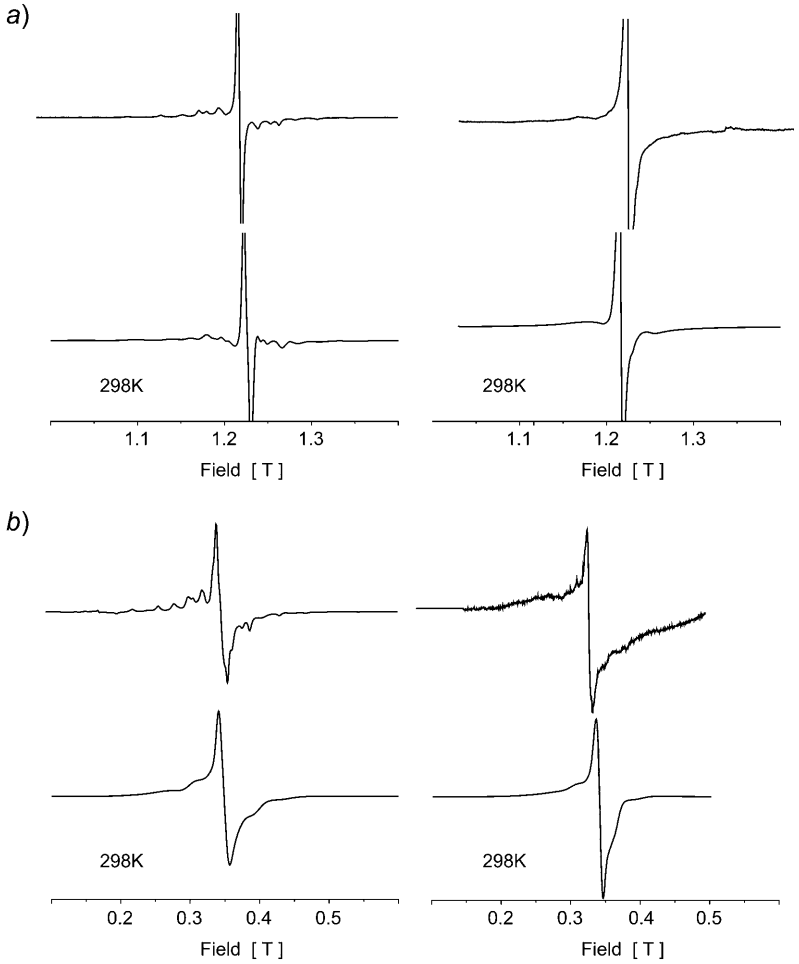


Fig. 5. *Experimental* (upper) *and simulated* (lower) *EPR spectra of magnetically dilute powders of* $[Y(DTPA)(H_2O)]^{2-}$ (left) *and* $[Y(DOTA)(H_2O)]^{-}$ (right) *with* ca. *1%* (w/w) $Gd^{III}$ a) *at the Q-band and* b) *at the X-band*

Contrary to our working hypothesis, the magnitude of the transient ZFS parameters $\sigma D$ and $\sigma E$ remains significant in powders, especially for the DOTA complex (*Table 1*). This could be a consequence of the sample preparation. The lyophilization procedure used may hinder the formation of ordered unit cells. In addition, the slight excess of ligand molecules can induce disorder in the final solid, leading to a distribution of ZFS parameters.

As it was described in previous studies, the transient ZFS modulation can be regarded as a dynamic equivalent of the strain observed in powders and frozen solutions [33]. By using the current definition of the strain parameters (full width at 0.6065 height of the *Gaussian* distribution), the transient ZFS strength in *Rast*'s

approach, $a_{2T}$, is given by *Eqn. 3*. Similarly, the second-order-term parameter of the static ZFS strengths, $a_2$, is given by *Eqn. 4*.

$$a_{2T} = [2/3(\sigma D/2)^2 + 2(\sigma E/2)^2]^{1/2} \quad (3)$$

$$a_2 = [2/3D^2 + 2E^2]^{1/2} \quad (4)$$

It is now possible to compare the values of $a_2$ and $a_{2T}$ measured for $[Gd(DTPA)H_2O]^{2-}$ and $[Gd(DOTA)\ H_2O]^-$ in powders, glasses, and liquid solutions (*Table 2*). For both complexes, $a_2$ calculated from the glassy samples is similar to that obtained from relaxation studies in aqueous solution [9][27]. However, the calculated static and transient ZFS in powders are significantly different. Thus, we show that the determination of ZFS parameters in glassy samples yields results more relevant to the problem of electron-spin relaxation in aqueous solution than those obtained in powders. This finding is quite reasonable if we consider that the environment of the $Gd^{III}$ complexes in frozen $H_2O$/glycerol mixtures is much closer to that in an aqueous solution than that of powders.

Table 2. *The ZFS Parameters of $[Gd(DTPA)H_2O]^{2-}$ and $[Gd(DOTA)H_2O]^-$ Determined by* Rast*'s Method in Solution, in Comparison with the Parameters Obtained from Glasses and Powders*

| | $[Gd(DTPA)(H_2O)]^{2-}$ | | | $[Gd(DOTA)(H_2O)]^-$ | | |
|---|---|---|---|---|---|---|
| | powder[a]) | frozen solution[b]) | aq. solution[c]) | powder[a]) | frozen solution[b]) | aq. solution[c]) |
| $a_2/10^{10}\ s^{-1}$ | 0.46 | 0.80 | 0.92 | 0.49 | 0.30 | 0.35 |
| $a_{2T}/10^{10}\ s^{-1}$ | 0.04 | 0.22 | 0.43 | 0.20 | 0.23 | 0.43 |

[a]) This work. [b]) [27]. [c]) [9].

EPR Spectra of powders of the macromolecular DOTA-derived gadolinate P792 in its isomerically pure racemic form P792(B) and as the mixture P792(R) of six stereoisomers were measured at 240 GHz and at the Q- and X-bands from 5 K to 298 K. Experimental and fitted spectra of both compounds in frozen solutions and powders are compared in *Fig. 6*. As for the powders of the DTPA and DOTA complexes, the high-frequency low-temperature spectra were fitted by adjusting the four ZFS parameters $D$, $E$, $\sigma D$, and $\sigma E$ (*Table 3*). Experimental and simulated spectra at the Q- and X-bands and 298 K are presented in *Fig. 7*. In contrast to what we observed for the DOTA complex, no broadening of the spectra at 240 GHz and 4 K is noticeable in powders of both macromolecular complexes reflecting a minimal change in the magnitude of $D$ values. However, for both complexes, the sign of $D$ is the opposite in powders as compared to glasses, indicating a change in structure, similar to that observed for $[Gd(DOTA)(H_2O)]^-$. Again, this sign change appears unambiguously in the experimental spectra at high frequency and low temperature (*Fig. 6*). The values of the strain $\sigma D$ and $\sigma E$ are in powders as large as in frozen solutions. Powders of the gadolinate complexes P792 were also prepared by the lyophilization procedure, and as it was mentioned for the DTPA and DOTA complexes, the large values of strain could be attributed to the sample preparation.

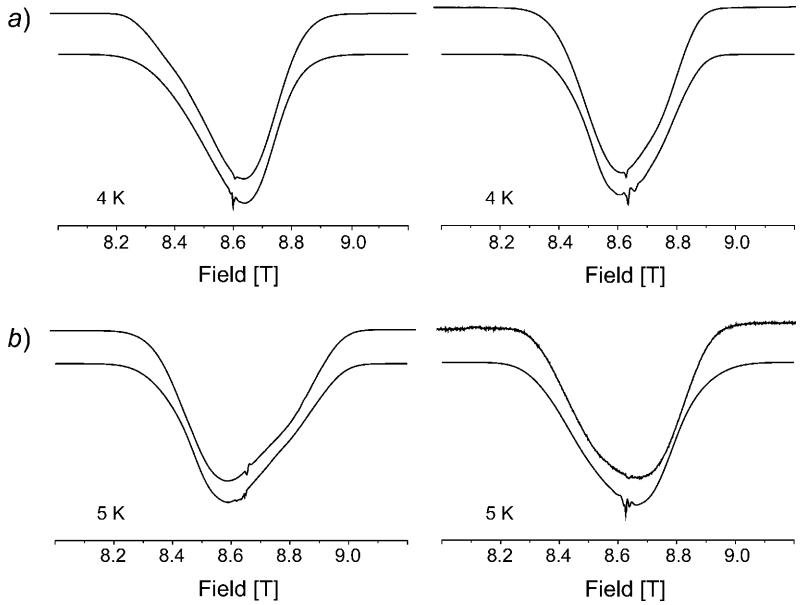


Fig. 6. *Experimental* (upper) *and fitted* (lower) *EPR spectra at 240 GHz of* a) *the gadolinate glasses P792(B)* (left) *and P792(R)* (right) *and* b) *the gadolinate powders P792(B)* (left) *and P792(R)* (right)

Table 3. *The ZFS Parameters of Gadolinates P792(B) and P792(R) Obtained by Fitting the Experimental EPR Spectra at 4 K and 240 GHz.* Estimated error is equal to 0.002 $cm^{-1}$

| | P792(B) | | P792(R) | |
|---|---|---|---|---|
| | powder | glass[a]) | powder | glass[a]) |
| $D$ [$cm^{-1}$] | 0.055 | − 0.060 | − 0.035 | 0.033 |
| $E$ [$cm^{-1}$] | 0.011 | 0.000 | 0.010 | 0.010 |
| $E/D$ | 0.20 | 0.00 | − 0.26 | 0.30 |
| $\sigma D$ [$cm^{-1}$] | 0.045 | 0.060 | 0.029 | 0.016 |
| $\sigma E$ [$cm^{-1}$] | 0.023 | 0.010 | 0.013 | 0.013 |

[a]) [27].

Our results show that powders of $Gd^{III}$ complexes with cyclic ligands prepared by a lyophilization procedure suffer from disorder similar to frozen solutions. Because this disorder is reflected by relatively large values of $\sigma D$ and $\sigma E$, the determination of the axial and rhombic parameters $D$ and $E$ is not easier than in glasses. Together with the small environment changes described above, it follows that experiments with powders of DOTA and DOTA-derived complexes show no additional advantages compared to those with frozen solutions.

Finally, we shortly discuss a possible extension of this work to further simplify the analysis. Spectra of single crystals should in principle lack both structural disorder and angular distribution and, therefore, allow to remove one more level of disorder from the sample. Thus, they offer an attractive route towards a precise, unambiguous

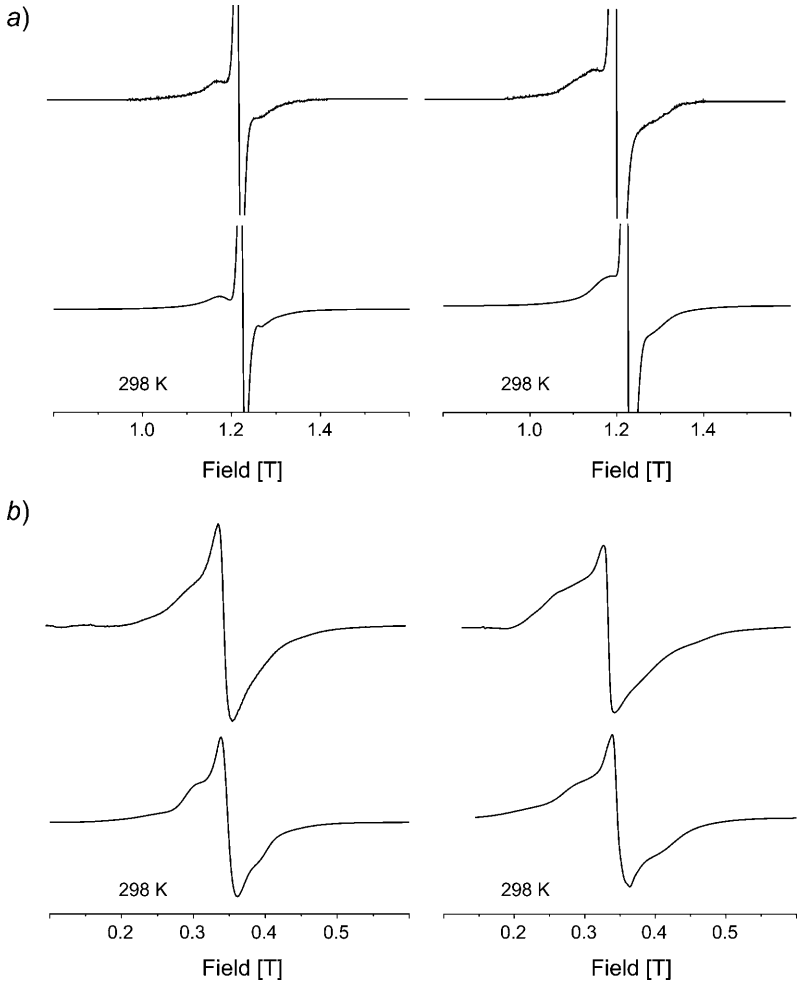


Fig. 7. *Experimental* (upper) *and simulated* (lower) *EPR spectra of the gadolinate P792 powders P792(B)* (left) *and P792(R)* (right) a) *at the Q-band and* b) at the *X-band*

determination of the static ZFS parameters $D$ and $E$, as well as higher-order terms. However, our results with powders suggest that such parameters might not be useful from the point of view of relaxation in liquids. Single-crystal results, besides the difficulty to obtain single crystals, are even more likely to suffer from structural differences compared to frozen and liquid solutions.

**Conclusions.** – Many $Gd^{III}$-based contrast agents for MRI have significant static ZFS which has a non negligible influence on the electronic relaxation of these compounds. The understanding of the origin of both the transient and the static ZFS will help to explain the relaxivity of $Gd^{III}$ complexes relevant as contrast agents for MRI. A first step towards this aim was accomplished thanks to the direct determination

of ZFS through performing high-field, high-frequency EPR measurements for several $Gd^{III}$ complexes in frozen solution. The static ZFS parameters in frozen solution were shown to be in good agreement with those obtained in aqueous solution. Lower-frequency measurements (X- and Q-bands) and spectral simulations for $[Gd(DTPA)(H_2O)]^{2-}$ and $[Gd(DOTA)(H_2O)]^{-}$ confirmed the soundness of the high-frequency results.

Contrary to what we expected, powder samples do not allow a more precise determination of the static ZFS parameters ($D$, $E$) by reducing the strain ($\sigma D$, $\sigma E$) due to disorder. EPR Experiments at multiple frequencies and variable temperature were performed with magnetically dilute $[Gd(DTPA)(H_2O)]^{2-}$, $[Gd(DOTA)(H_2O)]^{-}$, and the macromolecular DOTA-derived gadolinates P792(R) and P792(B), and showed that substantial disorder is present in the powders obtained by lyophilization. Furthermore, we observe significant differences on the ZFS of our powders compared to the frozen solutions, even including a systematic sign reversal of $D$. The main conclusion for both frozen solutions and powders is that the results obtained in glasses are more relevant to the problem of electron-spin relaxation in aqueous solution. Finally, high-field-EPR technique combined with very low temperature in frozen solution turned out to be the more appropriate technique to determine accurately the magnitude of the ZFS parameters and more specifically the sign of the axial ZFS parameter $D$.

The authors are grateful to the *Program Enhancement Grant 01-05* from the *FSU Foundation* to the *NHMFL EMR Program* for financial support. This work has been supported by the *Swiss National Science Foundation* and the *Swiss State Secretariat for Education and Research* (*SER*). This research was carried out in the frame of the *EU COST Action D38* and European founded *EMIL Program LSHC-2004-503569*. We are grateful to Dr. *Cyrille Denarie* (EPFL) for his help with the lyophilization procedure.

## REFERENCES

[1] A. E. Merbach, É. Tóth, 'The Chemistry of Contrast Agents in Medical Magnetic Resonance Imaging', 1st edn., John Wiley & Sons, Chichester, 2001, p. 471.
[2] P. Caravan, J. J. Ellison, T. J. McMurry, R. B. Lauffer, *Chem. Rev.* **1999**, *99*, 2293.
[3] G. M. Nicolle, É. Tóth, K.-P. Eisenwiener, H. R. Mäcke, A. E. Merbach, *J. Biol. Inorg. Chem.* **2002**, *7*, 757.
[4] L. Helm, A. E. Merbach, *Chem. Rev.* **2005**, *105*, 1923.
[5] Z. Jászberényi, A. Sour, É. Tóth, M. Benmelouka, A. E. Merbach, *Dalton Trans.* **2005**, 2713.
[6] E. Strandberg, P.-O. Westlund, *J. Magn. Reson., Ser. A* **1996**, *122*, 179.
[7] R. B. Clarkson, A. I. Smirnov, T. I. Smirnova, H. Kang, R. L. Belford, K. Earle, J. H. Freed, *Mol. Phys.* **1998**, *95*, 1325.
[8] S. Rast, P. H. Fries, E. Belorizky, *J. Chem. Phys.* **2000**, *113*, 8724.
[9] S. Rast, A. Borel, L. Helm, E. Belorizky, P. H. Fries, A. E. Merbach, *J. Am. Chem. Soc.* **2001**, *123*, 2637.
[10] T. Nilsson, J. Kowalewski, *Mol. Phys.* **2000**, *98*, 1617.
[11] S. Rast, P. H. Fries, E. Belorizky, A. Borel, L. Helm, A. E. Merbach, *J. Chem. Phys.* **2001**, *115*, 7554.
[12] D. Kruk, T. Nilsson, J. Kowalewski, *Phys. Chem. Chem. Phys.* **2001**, *3*, 4907.
[13] M. Benmelouka, A. Borel, L. Moriggi, L. Helm, A. E. Merbach, *J. Phys. Chem. B* **2007**, *111*, 832.
[14] A. Borel, J. F. Bean, R. B. Clarkson, L. Helm, L. Moriggi, A. D. Sherry, M. Woods, *Chem. – Eur. J.* **2008**, *14*, 2658.
[15] E. Belorizky, P. H. Fries, L. Helm, J. Kowalewski, D. Kruk, R. R. Sharp, P.-O. Westlund, *J. Chem. Phys.* **2008**, *128*, 052307.

[16] G. E. Uhlenbeck, L. S. Ornstein, *Phys. Rev.* **1930**, *36*, 823.
[17] W. Froncisz, J. S. Hyde, *J. Chem. Phys.* **1980**, *73*, 3123.
[18] W. R. Hagen, D. O. Hearshen, R. H. Sands, W. R. Dunham, *J. Magn. Res.* **1985**, *61*, 220.
[19] B. Cage, A. K. Hassan, L. Pardi, J. Krzystek, L.-C. Brunel, N. S. Dalal, *J. Magn. Reson., Ser. A* **1997**, *124*, 495.
[20] D. Mustafi, E. V. Galtseva, J. Krystek, L.-C. Brunel, M. W. Makinen, *J. Phys. Chem. A* **1999**, *103*, 11279.
[21] G. Lassmann, M. Kolberg, G. Bleifuss, A. Graslund, B. M. Sjoberg, W. Lubitz, *Phys. Chem. Chem. Phys.* **2003**, *5*, 2442.
[22] S. Cannistraro, *J. Phys. (Paris)* **1990**, *51*, 131.
[23] A. Venturelli, M. A. Nilges, A. Smirnov, R. L. Belford, L. C. Francesconi, *J. Chem. Soc., Dalton Trans.* **1999**, 301.
[24] G. N. George, R. C. Prince, R. E. Bare, *Inorg. Chem.* **1996**, *35*, 434.
[25] A. J. Pierik, W. R. Hagen, W. R. Dunham, R. H. Sands, *Eur. J. Biochem.* **1992**, *206*, 705.
[26] A. Seidel, H. Bill E., L., P. Nordblad, F. Kilar, *Arch. Biochem. Biophys.* **1994**, *308*, 52.
[27] M. Benmelouka, J. Van Tol, A. Borel, M. Port, L. Helm, L. C. Brunel, A. E. Merbach, *J. Am. Chem. Soc.* **2006**, *128*, 7808.
[28] M. Randin, G. Brunisholz, *Helv. Chim. Acta* **1959**, *42*, 1927.
[29] M. Port, C. Corot, O. Rousseaux, I. Raynal, L. Devoldere, J. M. Idée, A. Dencausse, *Magn. Reson. Mater. Phys. Biol. Med.* **2001**, *12*, 121.
[30] J. van Tol, L.-C. Brunel, R. J. Wylde, *Rev. Sci. Instrum.* **2005**, *76*, 74101.
[31] A. M. Portis, *Phys. Rev.* **1955**, *100*, 1219.
[32] J. Van Tol, EPRCALC National High Magnetic Field Laboratory, Tallahassee, FL, USA, 2005.
[33] A. Borel, R. B. Clarkson, R. L. Belford, *J. Chem. Soc.* **2007**, *126*, 054510.

*Received March 31, 2009*